Epimerization and Hydrolysis of Dalvastatin, a New Hydroxymethylglutaryl Coenzyme A (HMG-CoA) Reductase Inhibitor

Chong Min Won[1]

Received April 14, 1993; accepted August 2, 1993

In aqueous solutions, dalvastatin (1) undergoes epimerization as well as hydrolysis. The transformation of the drug was studied as a function of pH at 25°C in aqueous solutions containing 20% acetonitrile. At all pH values, first-order plots for the conversion are biphasic, indicating rapid equilibration of 1 with its epimer (2) and slower hydrolysis of 1 to the corresponding β-hydroxy acid (3). Apparent first-order rate constants for the biexponential equation are given as a function of pH. The alkyl–oxygen cleavage of the lactone ring results in the epimerization of 1 to 2, whereas the acyl–oxygen cleavage results in the hydrolysis of 1 to 3. The epimerization is an S_N1 reaction reaching an equilibrium of $[1]_{eq}/[2]_{eq} = 1.27$. The epimerization rate is increased with an increase in the water content of the solvent. The hydrolysis of 1 to 3 is acid and base catalyzed. The hydrolysis is reversible in acidic media and irreversible in neutral and basic media. At pH values greater than 9, the hydrolysis reaction proceeds more rapidly than the epimerization.

KEY WORDS: dalvastatin; hydroxymethylglutaryl coenzyme A (HMG-CoA) reductase inhibitor; epimerization; hydrolysis; kinetics.

INTRODUCTION

Dalvastatin (1 in Scheme I), (4*R*,6*S*)-6-[(E)-2-[2-(4-fluoro-3-methylphenyl)-4,4,6,6-tetramethyl-1-cyclohexenyl]vinyl]-4-hydroxy tetrahydropyran-2-one, is a potent inhibitor of cholesterol biosynthesis and is currently being developed for the treatment of hypercholesterolemia (1,2). Hydroxymethylglutaryl coenzyme A (HMG-CoA) reductase inhibitors competitively inhibit the enzyme HMG-CoA reductase, the rate-limiting enzyme in the biosynthesis of cholesterol (3). Dalvastatin is a prodrug and is itself an inactive lactone. After oral ingestion, the drug is hydrolyzed *in vivo* to the corresponding β-hydroxy acid (3), which is the pharmacologically active form (4). The possible clinical use makes it desirable to determine kinetic data on its reactivity in aqueous solutions. The drug undergoes epimerization to 2 as well as hydrolysis to 3. This paper describes the quantitative transformation of 1 in aqueous solutions as a function of pH for optimal design of appropriate dosage forms. The ease of the epimerization and hydrolysis also allows one to predict which species may appear in the body under physiological conditions.

[1] Analytical and Physical Chemistry Department, Rhône-Poulenc Rorer Central Research, Collegeville, Pennsylvania 19426-0107.

MATERIALS AND METHODS

Materials

The drug (1) and related compounds (2–4) were prepared by the Process Chemistry Department of Rhône–Poulenc Rorer Central Research. The purity of the synthesized compounds was greater than 99% as determined by HPLC analysis. Deionized and distilled water was used for the kinetic study. Acetonitrile was HPLC grade. All other chemicals were of ACS reagent grade and were used as received.

HPLC Analysis

The chromatography system consisted of a pump (Perkin Elmer 410), an automatic injector (Perkin Elmer ISS 100), a diode array detector (Perkin Elmer 480), and a networking computer system (Waters 860). The HPLC method employed a 250-mm × 4.6-mm-i.d., 5-μm-particle size, octyl-bonded silica stationary phase column which is sterically protected (Zorbax R_x–C_8) and a mobile phase consisting of acetonitrile: 0.007 *N* HCl (60:40, v/v). The flow rate was 1.5 mL/min and the detector wavelength for ultraviolet absorbance detection was 247 nm.

Kinetic Methods

Stock solutions of 1 (100 μg/mL) in acetonitrile and buffers (0.2 *M*) in water were prepared. Acetonitrile was needed because of the poor aqueous solubility of 1 (solubility of 1 in water, <1 μg/mL). A low buffer concentration of 0.02 *M* was used to minimize the possible general acid–base catalysis by the buffer species. In a typical kinetic experiment, 2 mL of the stock solution of 1, an appropriate amount of acetate (pH 4.3–5.5), phosphate (pH 6.2–7.8), or borate (pH 9.0–9.7) buffer stock solution, and an appropriate amount of 1 *M* NaCl to maintain an ionic strength of 0.1 were transferred to a 10-mL volumetric flask and filled to volume with water. For studies in HCl solutions, the stock solution was transferred to appropriately diluted HCl solutions (pH 1.3–2.3) containing NaCl. The apparent pH of the final solution containing 20% acetonitrile was measured. Solutions containing 20% acetonitrile were used in all kinetic experiments except those studying the effect of the acetonitrile concentration on the reaction rate.

Immediately after preparation, the kinetic solution was divided into HPLC vials and put on a thermostatted HPLC tray (Perkin-Elmer). The temperature of the solution was kept constant at 25.0°C (±0.5°C) using a refrigerated circulator (Fisher Scientific). The temperature of the solution in the vial was monitored using an electronic digital thermometer (Fisher Scientific). An aliquot (50 μL) of the sample in the vial was injected into the HPLC system every 20 min.

RESULTS AND DISCUSSION

Rate Constants

Using the HPLC conditions described previously, 1 and its related compounds (2–6) were separated (Fig. 1). The rate

0724-8741/94/0100-0165$07.00/0

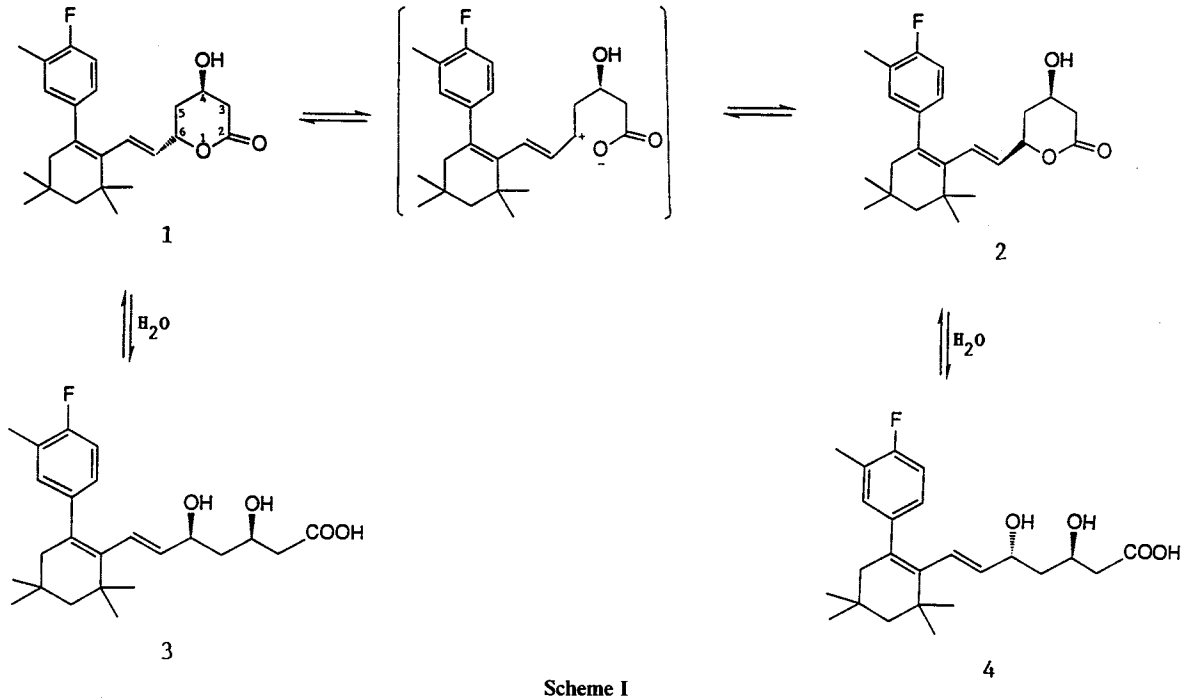

Scheme I

of loss of 1 in aqueous solutions at various pH values was monitored by HPLC. Typical semilogarithmic plots of the data obtained at various pH values are biphasic (Fig. 2), showing a rapid initial decrease in the peak area followed by a slower decrease. The biphasic curves were analyzed by feathering the data using a commonly employed method (5).

The peak area (A) of 1 conforms to the time (*t*) dependence of

$$A = A_a e^{-k_a t} + A_b e^{-k_b t} \quad (1)$$

The k_b values were estimated from the terminal linear slopes of such plots in accordance with

$$\log A = \log A_b - k_b t/2.303 \quad (2)$$

Where $\log A_b$ is the extrapolated intercept. The k_a values were estimated from the linear slopes of the feathered plots in accordance with

$$\log(A - A_b e^{-k_b t}) = \log A_a - k_a t/2.303 \quad (3)$$

where $\log A_a$ is the intercept of the semilogarithmic plots of the difference between the observed peak area and the antilogarithms of values obtained by the extrapolation of the terminal linear segment of the plot of log*A* vs time. The apparent first-order rate constants obtained are listed in Table I.

Effect of pH on the Reaction Rate

The log*k*–pH profiles for the apparent first-order rate

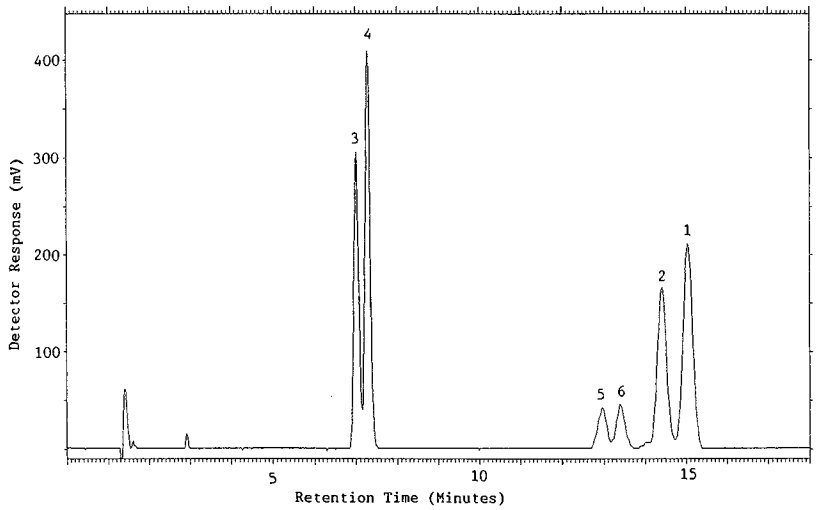

Fig. 1. HPLC chromatogram of 1 reacted at 25°C for 20 min in 0.02 *N* HCl containing 20% acetonitrile.

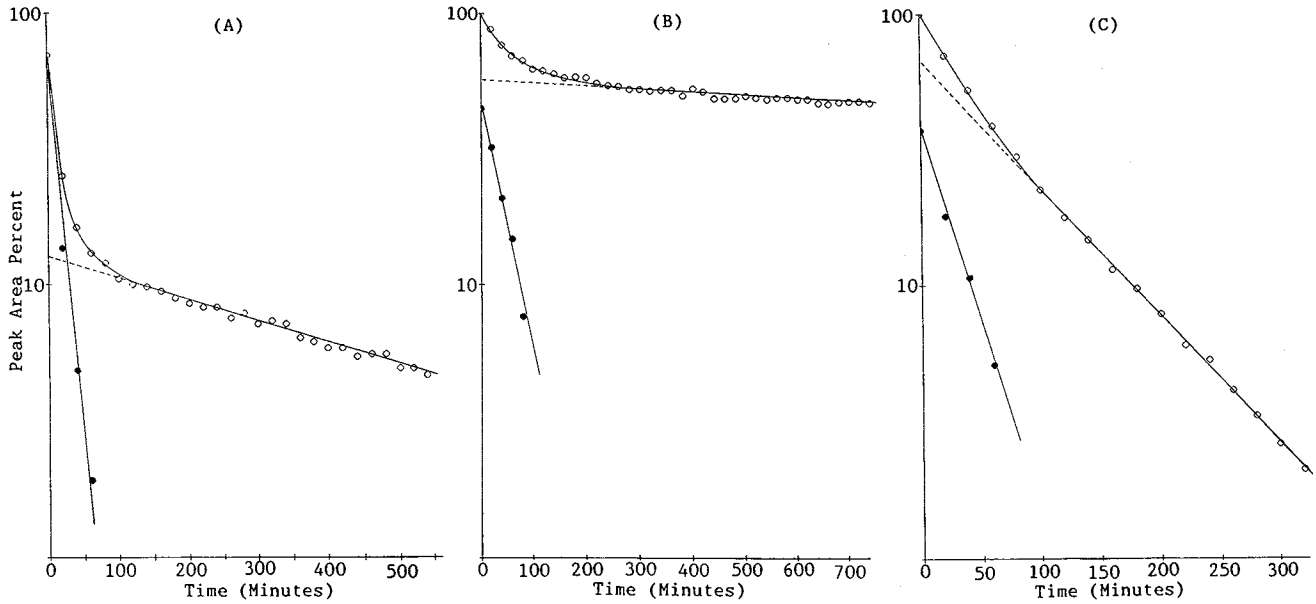

Fig. 2. Semilogarithmic plot (○) of peak area against time for the transformation of **1** at 25°C in buffer solutions containing 20% acetonitrile and the line (●) obtained by feathering. (A) pH 1.7; (B) pH 6.2; (C) pH 9.0.

constants for the epimerization (k_a) and hydrolysis (k_b) of **1** are given in Fig. 3. The log$k$–pH profile for k_a shows two distinct regions having a slope of approximately −1 in the acid region (pH below 3) and a broad plateau region above pH 2 in accordance with

$$k_a = k_H [H^+] + k_o \quad (4)$$

where $[H^+]$ is the activity of hydronium ion, and k_H and k_o are the catalytic rate constants for the hydronium-catalyzed and spontaneous reactions, respectively.

The log$k$–pH profile for k_b shows an additional region having a slope of approximately +1 above pH 7 in accordance with

$$k_b = k_H' [H^+] + k_o' + k_{OH}' [OH^-] \quad (5)$$

where $[OH^-]$ is the activity of hydroxyl ion, and k_H', k_o', and k_{OH}' are the catalytic rate constants for hydronium-, solvent-, and hydroxide-catalyzed reactions, respectively. The k_o and k_o' values were estimated from the plateau region of the respective profile.

The catalytic rate constants k_H, k_H', and k_{OH}' were estimated from the intercepts of the linear segments in accordance with

$$\log k_a = \log k_H - \text{pH} \quad (6)$$

and

Table I. Rate Constants (sec^{-1}) for the Transformation of Dalvastatin in Aqueous Solutions at 0.1 Ionic Strength and 25.0°C in Accordance with $A = A_a e^{-k_a t} + A_b e^{-k_b t}$

Medium[a]		pH[b]	$10^4 k_a$	$10^6 k_b$
[HCl]				
0.05		1.28	21.2	65.3
0.02		1.71	10.3	30.3
0.005		2.26	3.19	10.9
[CH_3COOH]	[CH_3COONa]			
0.016	0.004	4.33	2.76	3.88
0.01	0.01	4.98	3.21	2.53
0.004	0.016	5.55	2.78	2.28
[NaH_2PO_4]	[Na_2HPO_4]			
0.016	0.004	6.19	3.33	4.17
0.01	0.01	7.18	3.76	4.46
0.004	0.016	7.80	2.85	11.4
[H_3BO_3]	[NaOH]			
0.02	0.004	9.01	3.82	66.1
0.02	0.01	9.68	—	809

[a] Concentration (M) containing 20% acetonitrile.
[b] Apparent pH measured after adding 20% acetonitrile.

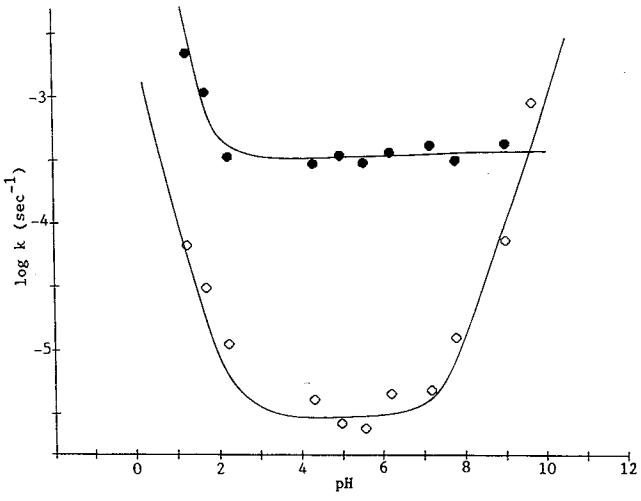

Fig. 3. The log$k$–pH profiles for transformation of **1** at 25°C in aqueous solution containing 20% acetonitrile, where the peak area can be expressed as $A = A_a e^{-k_a t} + A_b e^{-k_b t}$. The larger rate constant, k_a, was obtained by appropriate feathering of the plots of the logarithms of the peak area of **1** against time. k_a (●); k_b (○).

Table II. Catalytic Rate Constants, k_H, k_O, k_H', K_O', and k_{OH}' (sec^{-1}) for the Transformation of Dalvastatin in Aqueous Solutions in Accordance with $k_a = k_H[H^+] + k_O$ and $k_b = k_H' a_H + k_O' + k_{OH}'[OH^-]$

k_H	3.5×10^{-2}
k_O	3.3×10^{-4}
k_H'	1.3×10^{-3}
k_O'	3.2×10^{-6}
k_{OH}'	8

$$\log k_b = \log k_H' - pH \quad (7)$$

for the acid branch characterizing the hydronium attack on the drug molecule, or in accordance with

$$\log k_b = \log k_{OH}' - pK_w + pH \quad (8)$$

for the alkaline branch characterizing the hydroxide attack on the molecule. Assuming $pK_w = 14$, the catalytic rate constants were estimated (Table II).

Transformation in the Neutral and Alkaline pH Regions

The semilogarithmic plots of the peak area vs time are distinctly biphasic, showing a rapid initial decrease in the peak area of 1, followed by a slower second phase (Fig. 2). In the neutral pH region, this decrease is accompanied by a rapid increase in the peak area of 2, which is followed by a slower production of 3 and 4 (Fig. 4). The same observation was made when 2 was reacted under the same conditions. In both cases, the concentration of 1 is higher than that of 2 throughout the slower reaction phase. Based on the experimental observation, it is possible to develop a reaction scheme for the epimerization and hydrolysis of 1 in neutral and alkaline pH regions as depicted in Scheme II.

Scheme II proposes that 1 readily equilibrates with 2 where the sum (k_a) of the forward (k_1) and backward (k_2) rate constants is given by the rate dependence of Eq. (4). At pH values greater than 2 (Table I),

$$k_a = k_1 + k_2 = 3.1 \times 10^{-4}\ sec^{-1} \quad (9)$$

The equilibrium was estimated (Fig. 4) to be

$$k_1/k_2 = [2]_{eq}/[1]_{eq} = 0.79 \quad (10)$$

Equations (9) and (10) permit estimates of $k_1 = 1.4 \times 10^{-4}$ sec^{-1} and $k_2 = 1.7 \times 10^{-4}$ sec^{-1}.

The rapid epimerization of 1 to 2 characterized by k_a is independent of pH in the neutral and alkaline pH regions, but the hydrolysis of 1 to 3 characterized by k_b is catalyzed by hydroxide ion (Fig. 3). Therefore, the rate of hydrolysis exceeds that of the epimerization above pH 9 (Fig. 3). The epimerization is overwhelmed by the hydrolysis and tends to be negligible at higher pH values (Fig. 5). The similar observation was made when 2 was converted to 1 and 4 at pH 9.

Transformation in the Acidic pH Region

The acid-catalyzed transformation of 1 to 2 was so rapid in 0.02 *N* HCl that approximately 25% of the drug was already transformed to 2 at the moment the drug was dissolved in the acid solution, rapidly reaching the equilibrium (Fig. 6)

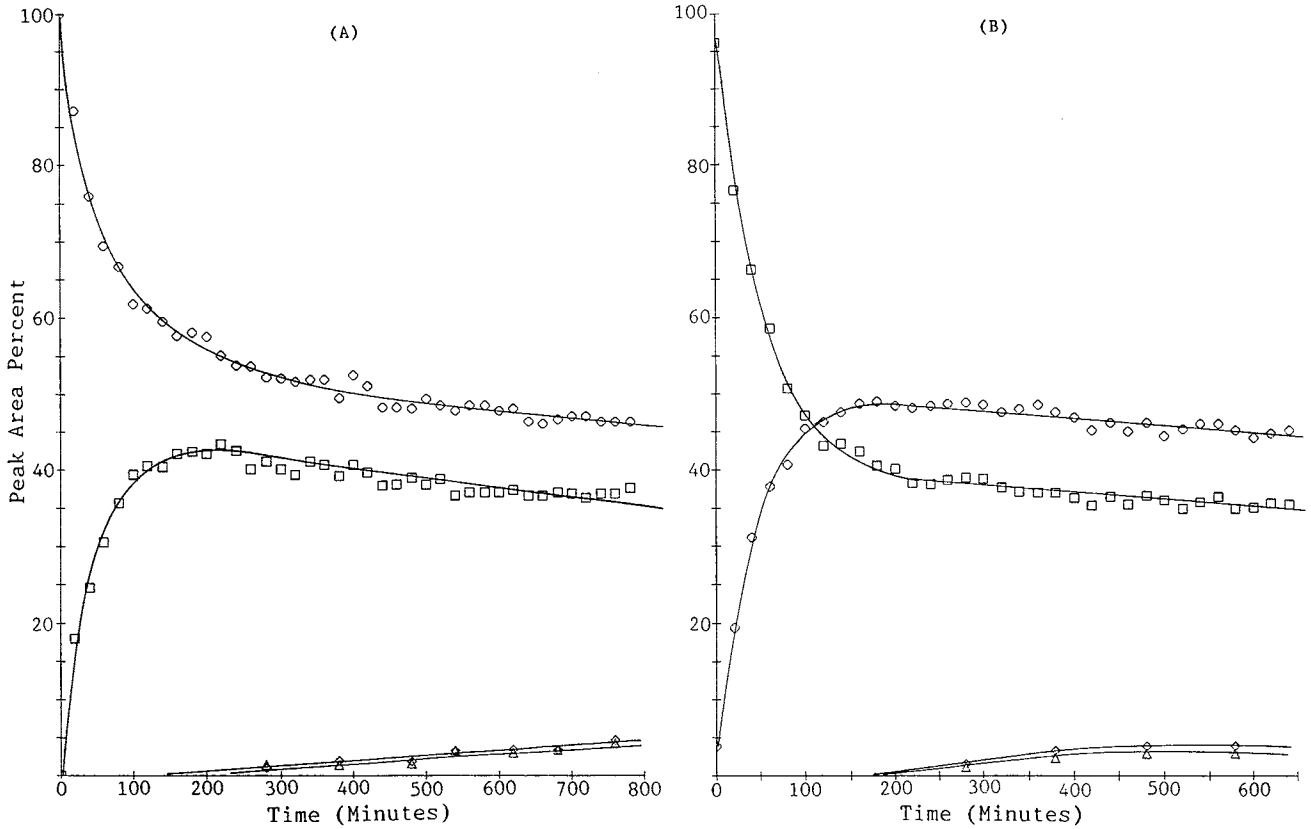

Fig. 4. Time course for 1 (○), 2 (□), 3 (△), and 4 (◇) during the transformation of 1 (A) and 2 (B) at 25°C in phosphate buffer of pH 6.2 containing 20% acetonitrile.

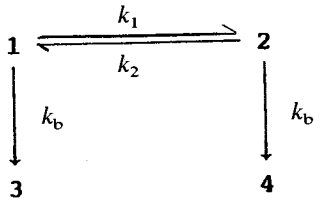

Scheme II

shown in Eq. (9). Similar results were obtained when 2 was reacted in the same medium.

In the pH region below 3, two additional unknown products were detected (Fig. 6). The same products were also observed when 2 was reacted under the same conditions. Liquid-chromatography–mass spectrometry (LC-MS) analysis of the unknowns (Fig. 1) showed both compounds to have a molecular ion of *m/z* 386. The diode array UV scan of the unknowns showed Peaks 5 and 6 to have λ_{max} values of 273 and 281 nm, respectively. The λ_{max} values are much higher than that (247 nm) of 1 or 2, indicating extended conjugated structures. Based on the limited information, the unknowns are predicted to be the dehydration products of the dihydroxy acids. The β-hydroxy acid (3) is stable in neutral and basic solutions, but it may undergo dehydration to 5 and 6 as well as lactonization to 1 in acidic solutions (Fig. 7).

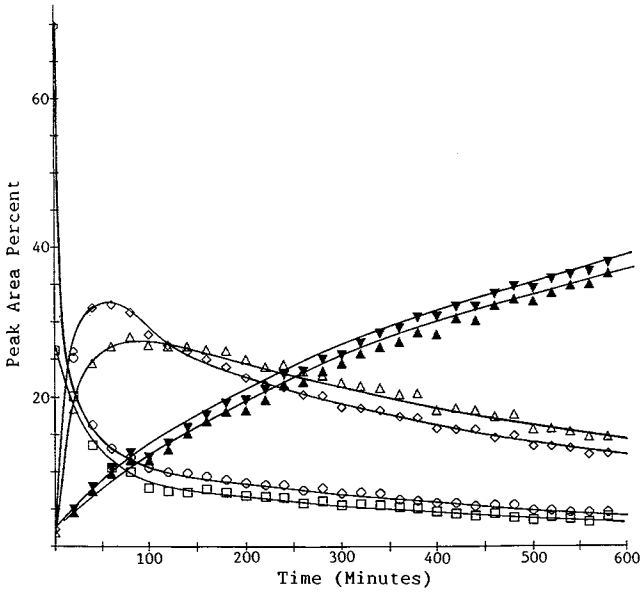

Fig. 6. Time course for 1 (○), 2 (□), 3 (△), 4 (◇), 5 (▲), and 6 (▼) during the transformation of 1 at 25°C in 0.02 *N* HCl (pH 1.7) containing 20% acetonitrile.

Effect of Organic Solvent on the Reaction Rate

Acetonitrile, which was added to keep the drug solubilized in kinetic solutions, has a significant effect on the reaction rate. The rate constant for the epimerization of 1 to 2 increased more than 10 times on decreasing the acetonitrile content in the medium from 30 to 15% (Table III). Immediately after dissolving the drug in a pH 6.2 phosphate buffer containing 10% acetonitrile, HPLC analysis of the drug solution showed 5% conversion of 1 to 2. After 20 min, 30% of 1 was converted.

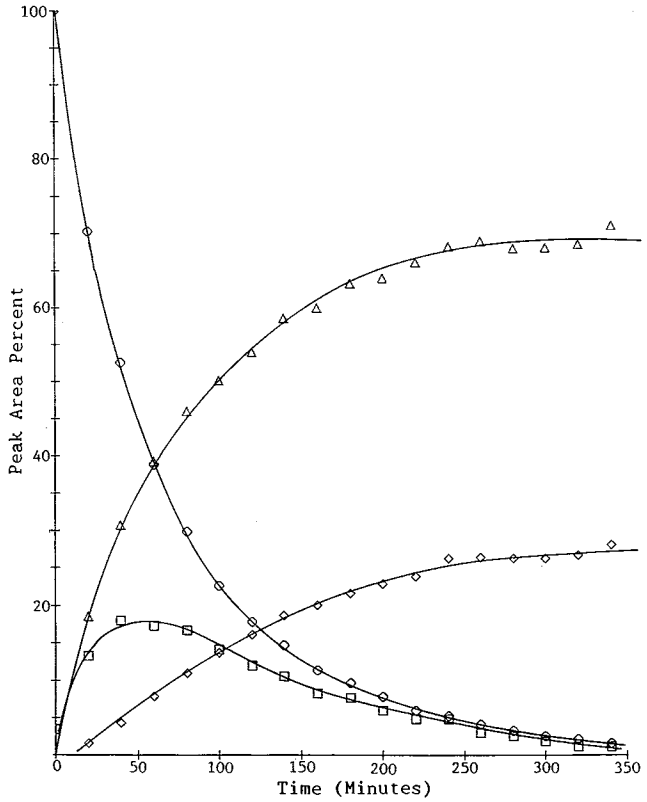

Fig. 5. Time course for 1 (○), 2 (□), 3 (△), and 4 (◇) during the transformation of 1 at 25°C in borate buffer, pH 9.0 containing 20° acetonitrile.

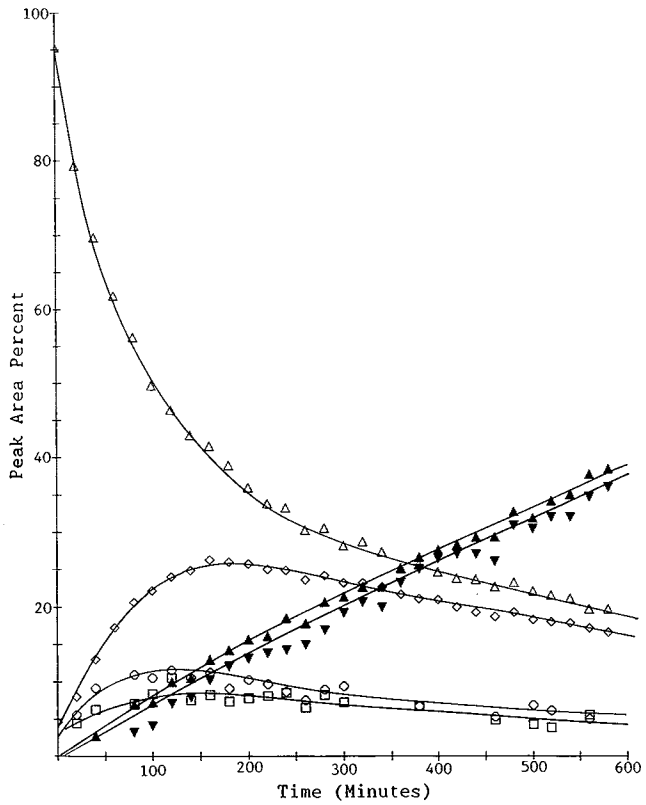

Fig. 7. Time course for 1 (○), 2 (□), 3 (△), 4 (◇), 5 (▲), and 6 (▼) during the transformation of 3 at 25°C in 0.02 *N* HCl (pH 1.7) containing 20% acetonitrile.

Table III. Effect of Acetonitrile Concentration on the Apparent First-Order Rate Constant in Phosphate Buffer, pH 6.2, in Accordance with $A = A_a e^{-k_a t} + A_b e^{-k_b t}$

% acetonitrile	$10^4 k_a$ (sec^{-1})	$10^6 k_b$ (sec^{-1})
10	8	4.88
15	8	4.65
20	3.3	4.17
25	1.4	3.87
30	0.67	0.97

Mechanism of Transformation

There are a number of paths by which loss of 1 may proceed. The paths may involve bond breakage at two possible sites, namely, the alkyl–oxygen and acyl–oxygen bonds of the lactone ring (Scheme I). In the alkyl–oxygen bond breakage, the reaction may be regarded as a nucleophilic substitution at the alkyl carbon (C-6), whereas in the acyl–oxygen breakage, it occurs at the acyl carbon (C-2). The acyl–oxygen cleavage is common and includes most ester hydrolyses, and the alkyl–oxygen cleavage is general for esters of tertiary alcohols and those secondary alcohols that yield the most stable carbonium ions (6). The alkyl–oxygen cleavage in dalvastatin is possible because the resultant carbonium ion is stabilized by the long conjugated resonance extending from the allylic group to the phenyl ring. For those lactones without an extended resonance system, obviously, the alkyl–oxygen cleavage is not possible (7,8).

The unimolecular cleavage of the lactone at the alkyl–oxygen bond is, in essence, an S_N1 reaction in which the carboxylate ion is the leaving group. An S_N1 reaction at C-6 would be expected to epimerize 1 to 2 because the carbonium ion is a flat sp^2 hybrid. When the carbonium ion is attacked by the carboxylate ion, it is equally likely to be attacked from either side. The rate of epimerization of 1 to 2, being an S_N1 reaction, is expected to be independent of OH^- concentration (Fig. 3). Because S_N1 processes are facilitated by the protonation of leaving groups, the acid catalysis is expected for the alkyl–oxygen cleavage. The epimerization rate was found to be very sensitive to the acetonitrile content in the media (Table III). As a charge is created when the carbonium ion is formed, the S_N1 reaction is expected to be favored by a polar medium.

The primary product in the alkaline hydrolysis of 1 is 3 (Fig. 5), whereas that of 2 is 4. The chirality is retained in the hydrolysis because the chiral centers are not involved in the acyl–oxygen cleavage. The carboxyl group in 3 is converted to the carboxylate ion in neutral and basic media, which, because of its negative charge, is not subject to a nucleophilic attack by OH^- at the C-6 carbon. Therefore, the hydrolysis of 1 to 3 is an irreversible reaction in the media.

ACKNOWLEDGMENTS

The author is grateful to Dr. S. Tang for LC-MS analysis and to Dr. C. Obetz for review of the manuscript.

REFERENCES

1. D. Amin, S. Gustafson, J. Weinacht, S. Cornell, K. Neuenschwander, B. Kosmider, A. Scotese, J. Regan, and M. Perrone. RG 12561, a novel, synthetic inhibitor of HMG CoA reductase and hypocholesterolemic agent that achieves high drug liver/plasma ratio. *Arteriosclerosis* **10**:828a (1990).
2. D. Amin and K. Neuenschwander. Dalvastatin. *Drugs Fut.* 17:377–379 (1992).
3. S. M. Grundy. HMG-CoA reductase inhibitors for treatment of hypercholesterolemia. *N. Engl. J. Med.* **319**:24–33 (1988).
4. V. K. Khetarpal, L. S. Storbeck, D. Wells, and R. H. Meacham. Method for separation and determination of lactone and hydroxy acid forms of a new HMG CoA reductase inhibitor (RG 12561) in plasma. *J. Chromatogr.* **567**:491–497 (1991).
5. A. A. Frost and R. G. Pearson. *Kinetics and Mechanism,* Wiley, New York, 1961, pp. 162–164.
6. E. S. Gould. *Mechanism and Structure in Organic Chemistry,* Holt, Rinehart and Winston, New York, 1962, p. 316.
7. E. R. Garrett and C. M. Won. Prediction of stability in pharmaceutical preparations. XVI. Kinetics of hydrolysis of canrenone and lactonization of canrenoic acid. *J. Pharm. Sci.* **60**:1801–1809 (1971).
8. M. J. Kaufman. Rate and equilibrium constants for acid-catalyzed lactone hydrolysis of HMG-CoA reductase inhibitors. *Int. J. Pharm.* **66**:97–106 (1990).